# FUSOGENIC ANTI-PSMA LIPOSOMES FOR ANTIVASCULAR CHEMOTHERAPY

**By**

**ANA MARIA GOMEZ**

**A thesis submitted to the**

**Graduate School-New Brunswick**

**Rutgers, The State University of New Jersey**

**in partial fulfillment of the requirements for the**

**Degree of Master of Science**

**Graduate Program in Biomedical Engineering**

**and**

**The Graduate School of Biomedical Sciences**

**University of Medicine and Dentistry of New Jersey**

**written under the direction of**

**Dr. Stavroula Sofou**

**and approved by**

_____

_____

_____

**New Brunswick, New Jersey**

***October 2013***

# ABSTRACT OF THE THESIS

## Fusogenic anti-PSMA Liposomes for Antivascular Chemotherapy

By ANA MARIA GOMEZ

Thesis Director: Dr. Stavroula Sofou

Since no treatment exists to cure advanced solid tumors, there is a growing need for innovative strategies to treat these patients. Antivascular therapy works by delivering therapeutics to tumor neovasculature to cut off blood supply and nutrients to the tumor, resulting in apoptotic or necrotic death. This study aims to selectively deliver to tumor vasculature adequate concentrations of the chemotherapeutic doxorubicin encapsulated in pH-tunable liposomes with doubly fusogenic properties for enhanced bioavailability. A PSMA (prostate specific membrane antigen)-targeting ligand is conjugated on the surface of liposomes to achieve high specificity to tumor endothelium, which uniquely expresses PSMA since normal endothelium is consistently PSMA-negative. A pH-responsive fusogenic peptide (GALA) is also attached on the liposome surface and remains masked during circulation of liposomes in the blood stream. Upon PSMA-mediated endocytosis of liposomes by tumor endothelial cells, pH acidification induces lipid phase-separation and domain formation on liposome membranes activating two fusion mechanisms — (1) the fusion peptides change their conformation from random coils to alpha-helices, become unmasked and available to interact with the endosomal membrane, and (2) the liposomal domain boundaries serve as sites to nucleate fusion with the endosomal membrane. As a result liposomes are expected to release the encapsulated cargo directly into the cytoplasm

of tumor endothelial cells, avoiding entrapment in the endosomal pathway. The first part of this study uses a parallel plate flow chamber to mimic blood flow conditions and measures binding and internalization of PSMA-targeting liposomal doxorubicin by prostate adenocarcinoma cells expressing varying levels of PSMA and human endothelial cells induced to express PSMA. The second part of this study aims to evaluate the membrane activity of GALA–labeled liposomes by varying membrane parameters. To monitor fusogenic activity, the self-quenching relief of a fluorescent dye encapsulated in endosomal-analogue vesicles incubated with GALA-labeled liposomes is measured. Since self-quenching is inversely proportional to content release, we observe that GALA-labeled liposomes exhibit pH-triggered membrane activity and induce content release of the endosomal analogues at late endosomal pH values.

## DEDICATION

Mami, Papi, Marcela, Alejandra, David, y Tia:

Gracias por enseñarme a ser la persona que soy hoy y por siempre creer en mí. Mis logros han sido posibles por el apoyo y la motivación que ustedes siempre me ofrecen.

Los quiero muchísimo.

# ACKNOWLEDGEMENTS

I sincerely wish to express my gratitude to the many people that have helped me reach this milestone. I especially want to acknowledge my advisor Dr. Sofou, thank you for your genuine guidance and assistance with my research and writing of this thesis. I would also like to thank my committee members, Dr. Francois Berthiaume and Dr. Charles Roth, for their continued support. In addition, thank you to Dr. Yarmush and the Biotech Training Program for their funding support and guidance.

Dr. Amey Bandekar, thank you for your patient mentoring and friendship. I also want to thank the current members of the lab: Michelle, Sally, Charles, and Trevan. You guys made me feel blessed to be a part of the “work family”. I wish you all the best and all the Starbucks coffee you can drink.

Without my friends in the Rutgers BME department, the time I spent in the graduate program would not have been as memorable. Renea, Dan M., Margot, and Jen: thank you for being such good friends and for the fun lunches, dinners, hiking trips, and New Brunswick outings.

Dan E., thank you for being supportive while I wrote this on our study dates and knowing just what to say to keep me motivated. I love that your positive outlook has been contagious.

Finally I would like to thank all of my family. Even though we are far away, I always feel your love and support. Thank you for your guidance and for molding me into the person I am today.

# TABLE OF CONTENTS

# LIST OF FIGURES

# LIST OF TABLES

# Chapter 1 INTRODUCTION

## 1.1 MOTIVATION AND SIGNIFICANCE

Cancer remains the second leading cause of death worldwide, as there is still no cure for advanced solid tumors. Patients with advanced stage solid tumors have a poor prognosis, resulting from highly recurrent tumors that are non-responsive to standard treatments such as immunotherapy, chemotherapy, or radiation [1]. Therefore there is a growing need for innovative strategies to treat these patients. A promising approach investigated is antivascular therapy, where the tumor vasculature is targeted to prevent the blood flow of oxygen and nutrients to the tumor, resulting in apoptotic or necrotic tumor cells [2]. Antivascular therapy is not envisioned as a monotherapy, but rather as adjuvant therapy that can be used in conjunction with primary strategies aimed at treating the cancer cells [3]. By taking this dual approach, it could be possible to obtain a synergistic effect in cancer treatment response.

Although antivascular therapy has been previously investigated, there have been few successes using this strategy and current treatments have resulted in increased side effects with minimal improvement over standard cancer therapies such as chemotherapy or radiation [4, 5]. This is due to inherent issues such as the inability to selectively target tumor vasculature, which results in toxicity to healthy tissue, and the inability to deliver therapeutically effective doses without resulting in systemic toxicity. These weaknesses are due to the choice of targeted moieties that are not uniquely expressed by tumor endothelium and the tendency of therapeutic agents to become entrapped within the delivery carriers or in subcellular compartments such as the endosome. To overcome these issues, a new approach is required which will selectively deliver adequate therapeutic concentrations directly to the cytosol of the tumor vasculature cells. The ultimate goal of this thesis is to design a new delivery system for antivascular therapy that has

the potential to hinder tumor blood flow to delay tumor growth in patients with advanced solid tumors.

## 1.2 LIPOSOMAL DELIVERY APPROACH

### 1.2.1 RATIONALE FOR LIPOSOMAL DELIVERY

Liposomes were selected as the vehicle to deliver therapeutics to the tumor vasculature for several motives including: nontoxicity of the carrier, controlled release of the therapeutic, and high drug-to-carrier ratio to transport sufficient quantities of the drug, in free form, to the tumor site.

Liposomes are vesicles composed of a lipid bilayer that can be designed to encapsulate a variety of therapeutics within the hydrophilic core or the hydrophobic membrane. The rationale for liposomal delivery further stems from their ability to passively accumulate within solid tumors due to the Enhanced Permeability and Retention (EPR) effect. The EPR effect states that the characteristically abnormal and leaky tumor vasculature results in enhanced uptake of nanoparticles at the tumor site when compared to healthy tissue [6]. Liposomal formulations such as Doxil®, polyethylene glycol (PEG)-coated liposomal doxorubicin, highly depend on this enhanced tumor vascular permeability for anticancer targeting [7]. Other liposomal formulations that are clinically approved for cancer therapy include liposomal cytarabine or daunorubicin [8]. However there are numerous liposomal anticancer drugs, such as liposomal cisplatin, in the clinical trial pipeline [9] as well as liposomal formulations with functionalized membranes to offer specific targeting to cancer cells [10]. Therefore to further increase bioavailability of therapeutics at the tumor site, this project exploits the passive accumulation from the EPR effect in combination with the ability to functionalize the liposomes with targeting moieties.

### 1.2.2 DESIGN OF ENVIRONMENTALLY RESPONSIVE MEMBRANES

Liposomes were additionally designed to undergo environmentally responsive release of the encapsulated therapeutic through the use of membrane heterogeneities. Depicted in Figure 1-1 are two types of membrane heterogeneities, and in bold is indicated the component of the phase-separating lipids that primarily contributes to the separation process: temperature can be used to induce heterogeneities through hydrocarbon tail interactions (a), whereas pH can be used as a trigger through lipid head group interactions (b).

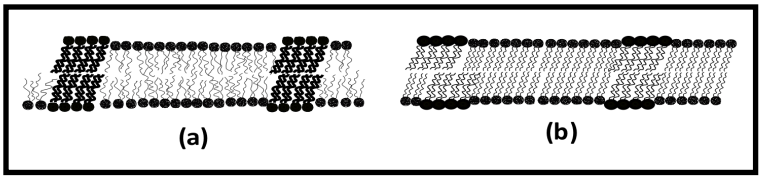


**Figure 1-1: ENVIRONMENTALLY RESPONSIVE MEMBRANE HETEROGENEITIES**
(a) Hydrocarbon tail interactions. (b) Lipid head group interactions.

In this thesis, pH-responsive liposomes were designed as previously discussed in the group's literature [11, 12]. Briefly, the membrane is comprised of a negatively charged lipid and a zwitterionic lipid. At neutral pH the electrostatic repulsion from the negatively charged lipid head groups creates a well-mixed (almost homogenous) membrane. When the pH becomes acidified - upon endocytosis of the liposome (pH < 5.0) or upon extravasation in the acidic tumor interstitium (pH < 6.5) - the negatively charged lipids become protonated resulting in the formation of lipid phase-separated domains driven by hydrogen bonding among the protonated titratable lipids. The outcome is a phase-separated membrane, where the defective phase boundaries can be used to release encapsulated therapeutics [13] or as sites to nucleate membrane fusion [14].

### 1.2.3 LIPOSOME FUSOGENICITY FOR ENDOSOMAL ESCAPE

A major barrier to successful nanoparticle delivery is the tendency of therapeutic agents to become entrapped within the carrier or cellular compartments such as the endosome [15]. This can result in decreased therapeutic efficacy as the drug can subsequently become degraded by lysosomal enzymes. To overcome this issue, liposomal membrane fusion with the endosomal membrane can be employed as an endosomal escape mechanism to release the therapeutic contents into the cytosol.

For this project the fusogenic potential of the heterogeneous membrane liposome is enhanced by the incorporation of a fusion peptide on the membrane surface. Specifically, the liposome is functionalized with a GALA fusion peptide [16] to fuse with the endosomal membrane. GALA is a synthetic 30-sequence amino acid peptide that was developed to study how viral fusion peptides interact with biological membranes. It contains a glutamic acid-alanine-leucine-alanine repeat to provide a pH-activated sequence. At neutral pH the peptide is in random coil formation due to electrostatic repulsion from the carboxylic acid residues on the glutamic acids. At acidic pH the glutamic acids are protonated resulting in an alpha helix conformational change, which is stabilized by intramolecular hydrogen bonding among the amino acids. In addition the hydrophobicity of the glutamic acid side chain increases and this hydrophobic face will preferentially bind to the endosomal membrane. Therefore the activated peptide spans the endosomal bilayer and can be utilized to avoid entrapment of therapeutics within the endosome and further degradation by the lysosome. Instead the therapeutic contents will be released directly into the cytosol to increase bioavailability and therapeutic efficacy.

## 1.3 ANTIVASCULAR THERAPY

### 1.3.1 RATIONALE FOR ANTIVASCULAR THERAPY

The blood supply of healthy tissues is efficiently regulated by pro-angiogenic and anti-angiogenic molecular factors, resulting in a highly organized vascular network. In contrast, aggressive neoplastic growth results in abnormal tumor vascularization which is oftentimes complex and immature [3]. The rationale behind antivascular therapy is the ability to target these intrinsic phenotypical differences between tumor-associated endothelial cells and healthy vasculature to prevent exposure of therapeutics to healthy tissue while delivering sufficient concentrations to the tumor site. Furthermore it has been shown that tumor growth and metastasis are highly dependent on tumor-associated blood vessels to sustain delivery of oxygen and nutrients to the tumor [2].

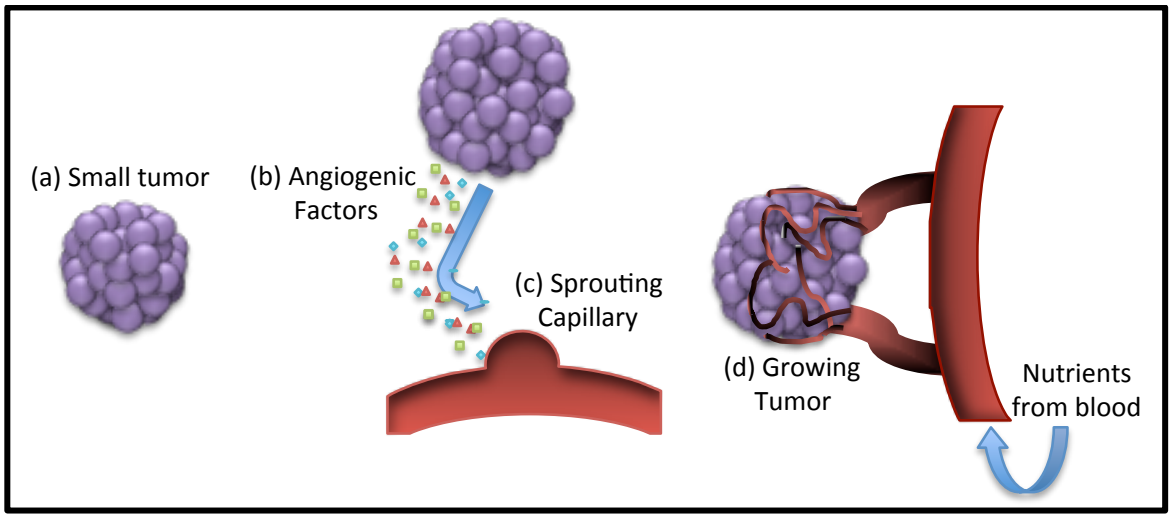


**Figure 1-2: TUMOR VASCULARIZATION PROCESS.**

Therefore targeting tumor-associated blood vessels to hinder tumor growth is considered a promising strategy. The two current approaches are: (1) targeting of angiogenic factors to prevent the formation of tumor vasculature through anti-angiogenic therapy and (2) targeting of existing tumor neovasculature through antivascular therapy [17].

### 1.3.2 PROSTATE SPECIFIC MEMBRANE ANTIGEN

This thesis will focus on the antivascular therapy approach by targeting Prostate Specific Membrane Antigen (PSMA), a marker that is uniquely expressed by tumor neovasculature of most advanced solid tumors including kidney, bladder, lung, breast, colorectal, and pancreatic [18]. Although there are several markers to target tumor neovasculature that are currently explored, such as Integrin $\alpha_v\beta_3$, vascular endothelial growth factor-receptor complexes, and endoglin [19], PSMA is a promising molecular target because it is not present in healthy endothelium thereby providing a target specific to tumor endothelium and the ability to spare healthy sites [20]. In addition although it is expressed in other tissues such as the salivary glands, small intestines, or brain, these sites would not be accessible by the circulating liposomes [21, 22]. PSMA-targeted therapies for cancer have sparked interest in the medical research community and first-generation products have already entered clinical trials, offering reasonable proof of concept. The approaches have varied from the use of recombinant proteins, nucleic acids, and cell-based strategies as well as drug-conjugated and radiolabeled anti-PSMA antibodies [23]. These initial studies have shown an absence of toxicity with responses in a minor portion of patients; however the doses necessary were near the maximum tolerated dose. Therefore a system to target PSMA while delivering a higher payload of the therapeutic without causing systemic toxicity could hold the key for antivascular treatment of advanced solid tumors.

## 1.4 PROJECT SCOPE

The objective of this thesis is to design and test a liposomal-based antivascular therapy that will overcome the weaknesses observed with current treatments: non-specific targeting of tumor vasculature, insufficient concentrations of therapeutics to the target site, and endosomal entrapment of therapeutics. To address these issues, a new class of liposomal drug carriers was

developed with the potential to maximize the therapeutic efficacy of antivascular treatments while sparing healthy sites.

The project is comprised of two sections to evaluate the efficacy of the anti-PSMA doubly fusogenic liposomes (Figure 1-3). The first section will focus on targeted delivery of a therapeutic to tumor vasculature using anti-PSMA functionalized liposomes under static and flow setups to mimic biological conditions. The second section will focus on evaluating the fusogenicity of GALA functionalized liposomes by systematically varying properties of the targeting membrane.

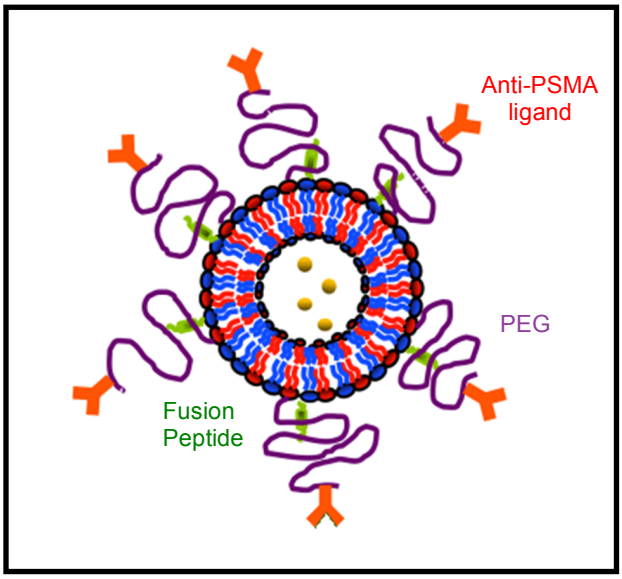


**Figure 1-3: ANTI-PSMA FUSOGENIC LIPOSOME DESIGN**

# Chapter 2 ANTI-PSMA TARGETING OF TUMOR NEOVASCULATURE

## 2.1 RATIONALE

As discussed in Chapter 1, the selection of PSMA as a molecular target for our delivery system arises from its unique expression in tumor vasculature and not healthy endothelium. Because PSMA is expressed in most solid tumors, the system can be used to treat a variety of cancers without modification. Taking these factors into consideration, the selection of a functional targeting ligand was dependent on its proven effectiveness through literature. The anti-PSMA monoclonal antibody J591 demonstrated acceptable toxicity and excellent targeting in a phase I clinical trial and was chosen for these purposes [18]. The treatment was well tolerated; moreover 74% of patients that received J591 had tumor vasculature that was effectively targeted as indicated through positive imaging. In the present study, a second targeting ligand, A10 aptamer, was chosen to compare the targeting effectiveness of both targeting ligands. The A10 aptamer is a synthetic oligonucleotide that was shown to demonstrate high PSMA affinity in vitro while exhibiting a higher target-to-blood ratio when compared to antibodies [24]. However unlike J591 antibody, no clinical studies have been performed using this RNA aptamer to date.

Doxorubicin is an anthracycline antibiotic, which works by intercalating DNA, and is commonly used to treat many types of cancers including: breast, adrenal cortex, endometrium, lung, and ovary [25]. In this thesis it was chosen as the proof-of-concept therapeutic because in its liposomal form it is widely used in the treatment against various solid tumors, and has an inherent fluorescence which can be exploited for assaying purposes. Since unencapsulated doxorubicin has been shown to induce cardiotoxicity [26, 27], liposomal formulations such as Doxil® have been utilized to decrease side effects and reduce this dose-limiting toxicity. Doxorubicin has also been shown to have an antivascular effect in solid tumors [28]. Because of

the above-listed qualities, doxorubicin was the drug of choice to incorporate in the delivery system.

For this section, assessment of PSMA targeting was performed in vitro; therefore cell lines expressing variable levels of PSMA were chosen to compare the extent of binding to receptor expression. LNCaP was chosen because of its high expression of PSMA and widespread use as a human prostate adenocarcinoma cell line [29]. In comparison MatLu, a rat prostate adenocarcinoma cell line [30] that expresses less PSMA (Figure 4-2), was selected because future work will study an in vivo model where MatLu cells are subcutaneously injected in rats to induce formation of tumors exhibiting vasculogenic mimicry whereby the 'vascular cells' express PSMA. In addition, the human umbilical vein endothelial cell (HUVEC) line [31] - that was induced to express PSMA after exposure to soluble tumor factors - was selected for these studies, since this in vitro model would most closely resemble antivascular therapy in vivo.

Finally, another important consideration for the in vitro flow setup was flow rate selection and the resulting shear rate. Although tumor blood flow is heterogeneous and dependent on tumor size, a flow rate of 0.1 mL/min was chosen for this primary study since this results in a shear rate of 15 $s^{-1}$, which is in the range of physiological shear rates observed in the tumor microcirculation [32].

## 2.2 OBJECTIVE

This study aims to determine the binding efficacy of two types of anti-PSMA ligands conjugated on pH-responsive vesicles as previously discussed. The binding efficacy is compared by measuring doxorubicin uptake in several cell lines to observe the effect of varying levels of PSMA expression. As negative controls, cell lines were incubated with liposomes not targeting PSMA (either without a targeting ligand or labeled with an isotype control antibody) to

determine if doxorubicin uptake was mediated through the PSMA-receptor. These studies are performed using a standard static setup as well as a flow setup to mimic the effect of blood flow conditions on targeting tumor vasculature.

## 2.3 HYPOTHESIS

PSMA-targeting ligands can be conjugated on pH-responsive liposomes to obtain 1) selective targeting of cell lines expressing PSMA under static and flow conditions and 2) selective and enhanced doxorubicin uptake by cell lines.

Additional hypothesis to be tested:

- Doxorubicin uptake will be greater in cells exposed to J591 antibody-labeled liposomes when compared to cells exposed to A-10 aptamer-labeled liposomes.
- PSMA-targeting under biomimetic flow conditions will result in a decrease in doxorubicin uptake when compared to the static experimental setup across cell lines.

## 2.4 MATERIALS AND METHODS

### 2.4.1 MATERIALS

The lipids 1,2-diheneicosanoyl-*sn*-glycero-3-phosphocholine (21PC), 1,2-distearoyl-sn-glycero-3-phosphate (monosodium salt) (DSPA), 1,2-distearoyl-*sn*-glycero-3-phosphoethanolamine-N-[PDP(polyethylene glycol)2000](ammonium salt) (PDP-PEG), 1,2-distearoyl-sn-glycero-3-phosphoethanolamine-N-[methoxy(polyethylene glycol)-2000] (ammonium salt) (DSPE-PEG), 1,2-distearoyl-*sn*-glycero-3-phosphoethanolamine-N-[carboxy(polyethylene glycol)-2000] (ammonium salt) (carboxyl-PEG), and 1,2-dioleoyl-*sn*-glycero-3-phosphoethanolamine-N-(7-nitro-2-1,3-enzoxadiazol-4-yl) (ammonium salt) (NBD-lipid) were purchased from Avanti Polar Lipids (Alabaster, AL) (all lipids at purity > 99%). The PSMA-targeting antibody J591 was

purchased from BZL Biologics, LLC (New York, NY). The RNA A10 PSMA aptamer (A10 aptamer) with the sequence 5"-NH2-spacer-GGGAGGACGAUGCGGAUCAGCCAUGUUUACGUCACUCCUUGUCAAUCCUCAUCGGCiT-3" containing 2"-fluoro pyrimidines, a 3"-inverted T cap, and a 5"-amino group attached by a hexaethyleneglycol spacer was purchased from Integrated DNA Technologies (Skokie, IL). BCA protein assay kit, 5,5'-dithiobis-(2-nitrobenzoic acid) (Ellman's reagent), dimethylformamide (DMF), and succinimidyl 4-[*p*-maleimidophenyl]-butyrate (SMPB) were purchased from Pierce (Rockford, IL). RPMI 1640 medium, EMEM, F-12K medium, Endothelial cell growth supplement (ECGS), and heparin sulfate, were purchased from ATCC (Manassas, VA). Matrigel™ and fetal bovine serum (FBS) was purchased from BD Biosciences (San Jose, CA). N-(3-dimethylaminopropyl)-N'-ethylcarbodiimide hydrochloride (EDC), N-hydroxysuccinimide (NHS), phosphate buffered saline (PBS), doxorubicin hydrochloride (DXR), ammonium sulfate, Sephadex G-50, Sepharose 4B, Sephadex PD10, Triton-X 100, ethylenediaminetetraacetic acid (EDTA), fibronectin from bovine plasma, and cholesterol were obtained from Sigma-Aldrich (Atlanta, GA).

### 2.4.2 VESICLE PREPARATION

Functionalized pH-tunable vesicles were composed of 21PC, DSPA, cholesterol, and DSPE-PEG (6:2:0.8:1.2 mole ratio). For antibody-conjugated vesicles, 16.7 mol% of the PEGylated lipid was PDP-PEG, while aptamer-functionalized vesicles contained 16.7 mol% carboxyl-PEG. Lipids were dissolved in chloroform and mixed in a 25 ml round bottom flask. The chloroform was evaporated under vacuum for ten minutes at 55°C using a Buchi rotavapor R-200 (Buchi, Flawil, Switzerland) to obtain a lipid film. To ensure dryness, the film was then exposed to $N_2$ stream for 5 minutes. This film was then hydrated with 1 ml of 250 mM ammonium sulfate (300 mOsm) and was allowed to become annealed for 2 hours at 55°C in a water bath. The lipid suspension

was then extruded 21 times through two stacked 200 nm polycarbonate membranes (Avestin Inc., Ottawa, Canada) in a water bath at 80°C. The lipid suspension was extruded again through 100 nm membranes. Vesicles were then passed through a 10 cm Sepharose 4B size exclusion chromatography (SEC) column and eluted with PBS (pH 7.4, 300 mOsm) to separate from the unentrapped ammonium sulfate. The average size of vesicle suspensions was measured by dynamic light scattering using a Zetasizer Nano Z590 (Malvern Instruments, Worcester, UK).

### 2.4.3 LOADING OF VESICLES WITH DOXORUBICIN

The ammonium sulfate gradient method was used for loading of doxorubicin into vesicles [33]. The prepared vesicles were incubated for 2 hours at 80°C with 1 mM doxorubicin in saline water (300 mOsm) at a 0.2:1 mole ratio of drug:lipid. After incubation, the suspension was quickly cooled in water to room temperature and unloaded doxorubicin was removed by SEC as described in the following paragraphs using different elution buffers depending on the subsequent conjugation chemistry.

### 2.4.4 CONJUGATION OF PSMA-TARGETING LIGANDS TO VESICLES

#### 2.4.4.1 J591 ANTIBODY CONJUGATION TO VESICLES

Unentrapped doxorubicin was removed from vesicles containing PDP-PEG via a Sepharose 4B column eluted with isosmolar PBS (pH 5.5) to a final (total) lipid concentration of 2 mM. The PDP groups on the PEG-chains were activated as previously described [11] by addition of 500 mM DTT (pH 5.5 in 300 mOsm PBS) at a 500:1 mole ratio of DTT:PDP followed by a 30 minute incubation on a shaker at room temperature. The vesicles were then separated from excess DTT by eluting the suspension with PBS pH 7.2 through a Sephadex G50 column. The antibody (0.1 mg) was activated by addition of 25 mM SMPB prepared in DMF at a 1:20 mole ratio of antibody: SMPB [11]. The antibody solution was then incubated on a shaker at room

temperature for 1 hour. After incubation, the solution was passed through a PD10 size exclusion chromatography (SEC) column eluted with isosmolar PBS at pH 7.2 to remove excess SMPB. The eluted solution was collected and a BCA protein assay was used to determine antibody presence. The activated antibody was then combined with the activated vesicles at a 1:111 mole ratio of antibody:PDP-lipid. The suspension was incubated overnight on a shaker at room temperature and vesicles were purified by SEC using a Sephadex G50 column eluted with isosmotic PBS (pH 7.4). The number of antibodies per vesicle was calculated using previously reported methods by quantifying the concentration of antibodies using a BCA protein assay and quantifying lipid concentration through fluorescence intensity for an average vesicle size as measured by light scattering [11].

#### 2.4.4.2 ISOTYPE CONTROL ANTIBODY CONJUGATION TO VESICLES

Isotype control antibody conjugation proceeded as described above using Herceptin® (Genentech, South San Francisco, CA) instead of J591 antibody. Herceptin® targets HER2-neu receptor, which is not expressed by these cell lines.

#### 2.4.4.3 A10 APTAMER CONJUGATION TO VESICLES

Unentrapped doxorubicin was removed from vesicles containing carboxyl-PEG via a Sepharose 4B column eluted with isosmolar 10 mM MES buffer (pH 6.0) to a final total lipid concentration of 2 mM. EDC and NHS solutions were prepared in UltraPure® distilled water (Life Technologies, Grand Island, NY). The carboxyl groups were activated by addition of 100 µl of 400 mM EDC followed by 100 µl of 100 mM NHS to 5 µmole total lipid. The suspension was then incubated for 30 minutes on a shaker at room temperature. To remove excess EDC and NHS, the solution was passed through a G50 column eluted with isosmolar MES buffer at pH 6.0. The eluted vesicles were collected and incubated with A10 PSMA-targeting aptamer at a 1:12.5 mole ratio of

aptamer: carboxyl-lipid overnight on a shaker at room temperature. The suspension was then passed through a Sepharose 4B column (eluted with PBS, pH 7.4, 300 mOsm) to exclude unconjugated aptamer. The number of aptamers per vesicle was calculated by quantifying the concentration of aptamers using a Quanti-iT™ RNA Assay Kit (Life Technologies, Grand Island, NY) and quantifying lipid concentration through fluorescence intensity for an average vesicle size as measured by light scattering.

### 2.4.5 CELL CULTURE

All cell lines (LNCaP, Mat-Lu, HUVEC, and MDA-MB-231) were obtained from ATCC (Manassas, VA). LNCAP and MatLu cells were propagated and maintained at 37°C in RPMI-1640 medium with 10% FBS, 100 units/ml penicillin, and 100 µg/ml streptomycin. HUVECs were propagated in F12-K medium supplemented with 0.05 mg/ml ECGS, 0.1 mg/ml heparin, 10% FBS, 100 units/ml penicillin, and 100 µg/ml streptomycin, and MDA-MB-231 cells were propagated in EMEM with 0.05 mg/ml ECGS, 0.1 mg/ml heparin, 10% FBS, 100 units/ml penicillin, and 100 µg/ml streptomycin.

### 2.4.6 INDUCING PSMA EXPRESSION IN HUVEC

HUVECs are induced to express PSMA by incubation on Matrigel™ with tumor-conditioned media (TCM) collected from the human breast carcinoma cell line MDA-MB-231 as previously described [31]. Briefly, MDA-MB-231 cells were grown to 100% confluency in a 225 $cm^2$ flask. The media was removed and fresh EMEM was added and then collected after 24 hours. TCM was centrifuged and the supernatant was sterile filtered and stored at -20 °C. HUVEC cells were then plated on Matrigel™ in TCM for 18 hours. PSMA-expression was then verified by immunohistochemistry using the J591 antibody followed by a secondary goat anti-mouse FITC-conjugated antibody [18].

### 2.4.7 TARGETING OF PSMA-EXPRESSING CELLS IN VITRO

#### 2.4.7.1 STUDIES UNDER STATIC AND FLOW CONDITIONS OF LIPOSOME UPTAKE BY LNCaP AND MatLu CELLS

Uptake of doxorubicin by LNCaP and MatLu in monolayers delivered by targeted and non-targeted pH-triggered lipid vesicles was monitored under flow and static conditions. Lipid vesicles were diluted in RPMI-1640 media at a final concentration of 0.06 µmol lipid/ml. Standard 1”x3” glass microscope slides (VWR Scientific Products, West Chester, PA) were pre-treated with a coat of 2 µg/mL fibronectin and incubated at 37 °C for three hours before use. Then 1.5 million cells were harvested and plated on the slide and incubated within a petri dish for two days before the experiment. The same quantity of cells was also plated onto a 1”x3” Lab-Tek II chamber slide (Nunc International, Wiesbaden-Biebrich, Germany) for the static condition. A rectangular parallel plate flow chamber (Glycotech, Gaithersburg, MD) was used with a gasket thickness of 0.01” and a flow path width of 1.0 cm. A constant flow rate of 0.1 ml/min was maintained using a PHD Ultra Syringe Pump (Harvard Apparatus, South Natick, MA) over the period of 1 to 6 hours at 37°C and 5% $CO_2$. For the static incubation conditions, the 0.01” height of vesicle suspension was kept constant for the same incubation period.

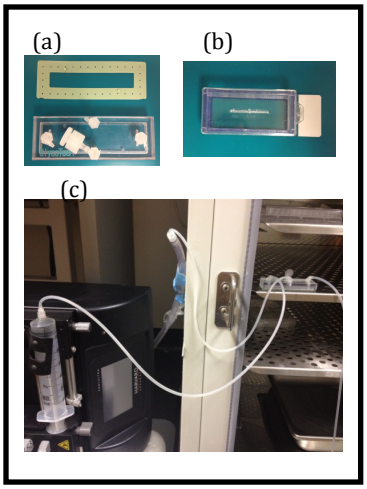


**Figure 2-1: FLOW AND STATIC EXPERIMENTAL SETUP**
(a) Parallel plate flow chamber and gasket (b) Static chamber slide and (c) Flow incubation setup.

#### 2.4.7.2 FLOW AND STATIC STUDIES ON HUVEC

For PSMA-expressing HUVEC the procedure varied slightly. The gasket was first placed on the glass microscope slides used for plating cells. The flow path area was then pre-coated with Matrigel™ before the HUVEC were plated using tumor-conditioned media. After 18 hours, the media was removed to prepare the slides for the flow study, which proceeded under the same conditions as above. For the static incubation, the Lab-Tek II chamber slide was also pre-coated with Matrigel™ before plating the HUVEC using tumor conditioned media. The cells were ready for incubation experiments with liposome-containing media after 18 hours.

#### 2.4.7.3 DOXORUBICIN QUANTIFICATION

After incubation with vesicles loaded with doxorubicin, cells were washed twice with PBS, resuspended in 500 µl of PBS, and counted using a hemocytometer. For total bound doxorubicin measurements (surface bound and internalized), the cells (in 0.5 ml) were lysed by addition of 0.5 ml distilled water and 100 µl of Triton-X 100 (5 % w/w) and sonicated for 10 minutes using a Branson 1510 water sonicator (Branson Sonic Power Co., Danbury, CT). To complete cell lysing, 2.4 mL of acidified isopropanol (90% isopropanol, 10% 12 N hydrochloric acid, v/v) was added to the sample [34]. For internalized doxorubicin measurements, the cells were resuspended in 500

µl of PBS and incubated with 1 ml of stripping buffer (50 mM glycine, 100 mM NaCl, pH 2.8) for 5 minutes in the dark at room temperature to remove surface bound vesicles. The cells were then washed twice with PBS and counted before being lysed as previously described. Doxorubicin fluorescence intensities were measured using a SLM AMINCO 8000 spectrofluorometer (SLM Instruments, Inc., Urbana, IL) and a 1 mm path length quartz cuvette (excitation 470 nm; emission 592 nm). Fluorescence was corrected by subtraction of scattered light from cell suspensions that were not exposed to lipid vesicles and contained equal cell densities. Finally, doxorubicin concentration in the samples was determined by fluorescence and doxorubicin uptake per cell was calculated.

## 2.5 STATISTICAL ANALYSIS

Results were reported as the arithmetic mean of n independent measurements ± the standard deviation. ANOVA followed by Tukey's post-hoc test were used to calculate significant differences in the behavior between the differently labeled vesicles for all cell lines studied. P-values less than 0.05 were considered to be significant.

## 2.6 RESULTS

### 2.6.1 VESICLE CHARACTERIZATION

The lipid vesicles used in this study were approximately 115 ± 8 nm (PDI = 0.1 ± 0.1) for all vesicle types (n=12). The antibody-conjugated vesicles contained 14 ± 2 antibodies per vesicle (n=5), whereas aptamer-conjugated vesicles contained 8 ± 3 aptamers per vesicle (n=6). Doxorubicin loading efficiency was 32 ± 7% for all liposome compositions (n=13).

### 2.6.2 CELL-ASSOCIATED DOXORUBICIN

As expected with increasing PSMA expression, there is an increase in doxorubicin uptake by cells. After 6 hours of incubation with J591-conjugated vesicles, the LNCaP cells under static conditions exhibit $67\times10^{-10}$ µmole doxorubicin/cell, which is 2.2 times more than MatLu cells (p=0.003) and 2.3 times more when compared to HUVECs (p=0.003). Higher doxorubicin uptake was also observed in LNCaP cells under flow conditions, showing 2.3 to 2.9 times greater uptake than MatLu cells and HUVECs (p=0.003, 0.002), respectively.

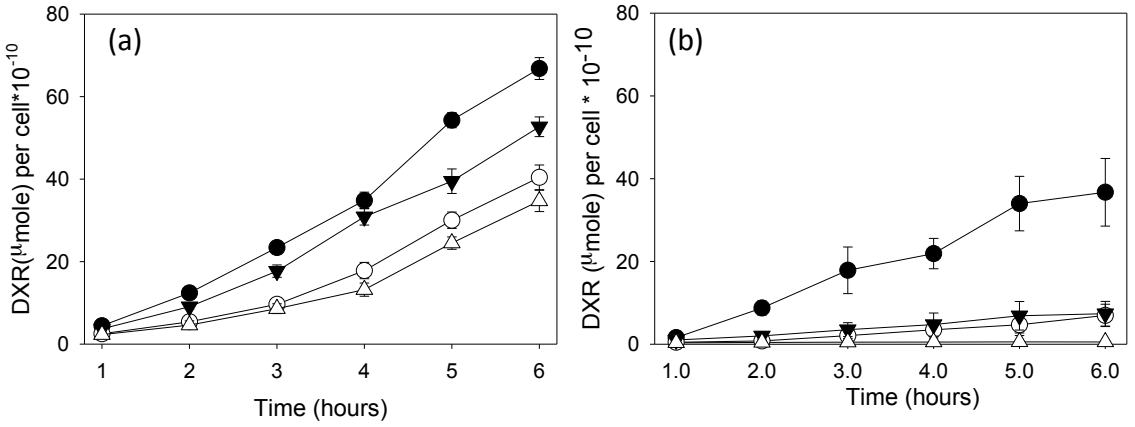


**Figure 2-2: LNCaP DOXORUBICIN UPTAKE**
The cells were exposed to anti-PSMA (a) J591 antibody and (b) A-10 aptamer - labeled liposomes. The doxorubicin quantity measured and incubation conditions are as follows: (●) total bound-static incubation conditions, (○) internalized-static incubation conditions, (▼) total bound under flow conditions (0.1 ml/min), and (Δ) internalized under flow conditions (0.1 ml/min).

After 6 hours, LNCaP cells exposed to J591 antibody-conjugated vesicles, Figure 2-2(a), exhibit a significant increase in doxorubicin uptake when compared to A-10 aptamer-conjugated vesicles under static and flow conditions (p=0.01, 0.002), Figure 2-2(b). At the same time point, LNCaP cells incubated under flow conditions resulted in a marked decrease of doxorubicin uptake when compared to cells incubated in static conditions for antibody-labeled vesicles (p=0.124) as well as aptamer-labeled vesicles (p=0.011).

The same trends for doxorubicin uptake of cells exposed to J591-labeled vesicles compared to A-10 aptamer-labeled vesicles were observed with MatLu cells (Figure 2-3) incubated under static (p=0.007) and flow conditions (p=0.019). MatLu cells incubated under flow conditions also resulted in a decrease of doxorubicin uptake when compared to cells incubated in static conditions. However results were not statistically significant for either antibody-labeled vesicles (p=0.214) or aptamer-labeled vesicles (p=0.898).

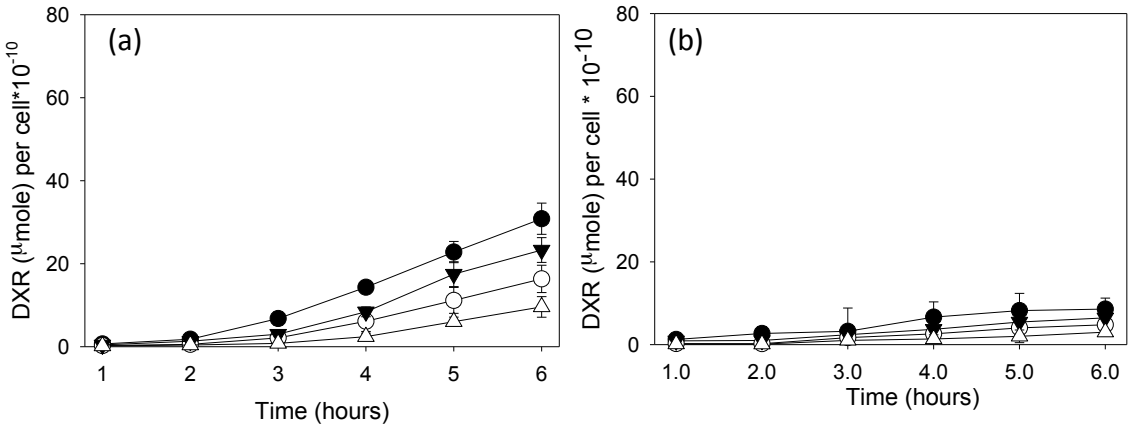


**Figure 2-3: MatLu DOXORUBICIN UPTAKE**
The cells were exposed to anti-PSMA (a) J591 antibody and (b) A-10 aptamer - labeled liposomes. The doxorubicin quantity measured and incubation conditions are as follows: (●) total bound-static incubation conditions, (○) internalized-static incubation conditions, (▼) total bound under flow conditions (0.1 ml/min), and (Δ) internalized under flow conditions (0.1 ml/min).

For PSMA-induced HUVEC (Figure 2-4), doxorubicin uptake was observed only when the cells were exposed to J591 antibody-labeled vesicles. In contrast, cells experienced minimal uptake of doxorubicin when exposed to A-10 aptamer-labeled vesicles.

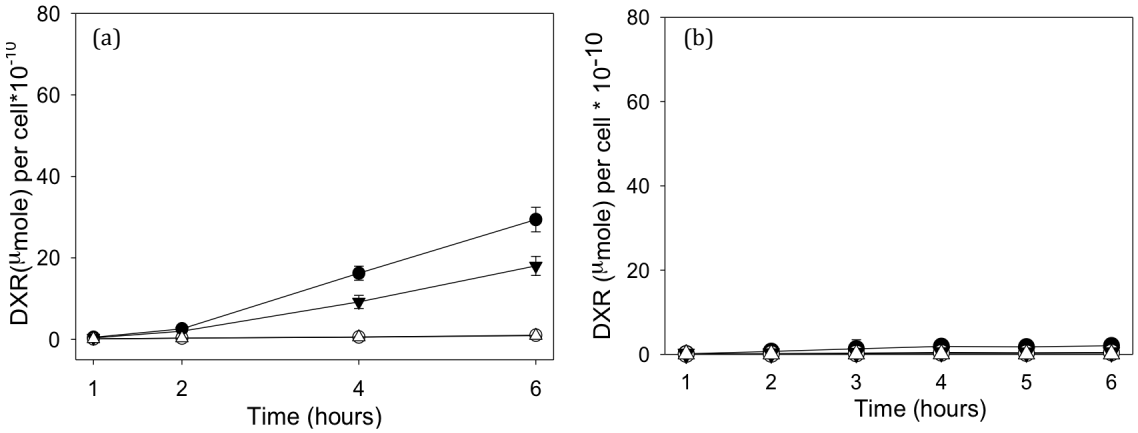


**Figure 2-4: HUVEC DOXORUBICIN UPTAKE**
The cells were exposed to anti-PSMA (a) J591 antibody and (b) A-10 aptamer - labeled liposomes. The doxorubicin quantity measured and incubation conditions are as follows: (●) total bound-static incubation conditions, (○) internalized-static incubation conditions, (▼) total bound under flow conditions (0.1 ml/min), and (Δ) internalized under flow conditions (0.1 ml/min).

The total bound and cell-internalized doxorubicin of each cell line for the antibody-conjugated vesicles is shown in Figure 2-2(a), Figure 2-3(a), and Figure 2-4(a). For the LNCaP cells under static condition at 6 hours, 61% of the total bound liposomes were internalized, followed by 53% by MatLu cells, and only 3% by HUVECs. In Figure 2-2(b), Figure 2-3(b), and Figure 2-4(b), the total bound and cell-internalized doxorubicin by cells exposed to the aptamer-conjugated liposomes is shown. For the aptamer-labeled vesicle case at 6 hours, LNCaP cells internalized 19% of the total bound liposomes.

As a negative control, the percentage of doxorubicin uptake by cells exposed to non-targeting liposomes either without a targeting ligand or conjugated with Herceptin® (an isotype control antibody which targets HER2-neu receptor not expressed by these cell lines) was measured.

**Table 1: DOXORUBICIN UPTAKE BY CELLS EXPOSED TO NON-TARGETING LIPOSOMES FOR 6 HOURS**

| **Incubation Condition** | **LNCaP cells (**μmole/cell * $10^{10}$) | **MatLu cell (**μmole/cell * $10^{10}$) |
|---|---|---|
| Static-No Targeting Ligand | 10.25 ± 0.21 | 4.57 ± 0.31 |
| Static-Irrelevant Antibody | 4.89 ± 0.45 | 3.28 ± 1.04 |
| Flow-No Targeting Ligand | 7.15 ± 0.21 | 3.77 ± 0.30 |
| Flow-Irrelevant Antibody | 2.44 ± 0.10 | 1.01 ± 0.35 |

Across cell lines, there was minimal uptake of non-targeting vesicles under both static and flow conditions at the longest incubation time of 6 hours (Table 1).

## 2.7 DISCUSSION

This section addressed the feasibility of conjugating anti-PSMA ligands on pH-sensitive vesicles to observe binding efficacy, by measuring doxorubicin uptake by PSMA-expressing cells. The study was performed over time, with the longest incubation period of 6 hours corresponding to an average half-life of pH-responsive liposomes previously studied by the group [11]. By measuring the total cell-bound doxorubicin as well as the cell-internalized doxorubicin, it was shown that anti-PSMA ligands conjugated on liposomes maintained their ability to target PSMA-expressing cells and effectively deliver doxorubicin to these cells lines.

The results showed a significant difference between doxorubicin uptake by cells exposed to J591-labeled liposomes compared to A-10 aptamer-labeled liposomes. Although aptamers have some potential advantages over antibodies including their economical and reproducible synthesis, the PSMA-targeting A-10 aptamer was not as effective as J591 antibody when conjugated on the liposomes. It is possible that this could be due to the aptamer having a lower affinity than the antibody. The immunoreactivity of each ligand upon conjugation to liposomes was not evaluated in this study, but the affinities of each free ligand are reported to be 1.83 nM for the antibody [35] and 520 nM for the aptamer [36]. In fact, second-generation A-10

aptamers have recently been synthesized to enhance binding activity and specificity of the aptamer [37].

This study was performed under static and flow conditions to allow for comparison between a commonly used static setup and a parallel plate flow chamber setup (Figure 2-1) which was chosen to provide a biomimetic in vitro testing system. This is especially important for antivascular therapy, where the tumor-associated endothelial cells will be exposed to targeting doxorubicin-loaded liposomes under vascular flow conditions. Therefore this study is able to observe how effectively the liposomes overcome the flow and shear environment to bind to the PSMA-expressing cells. As expected, PSMA-targeting under biomimetic flow conditions resulted in a decrease in doxorubicin uptake when compared to the static experimental setup. However there was still considerable doxorubicin uptake under flow conditions for LNCaP and MatLu cells. It is important to take the flow environment into consideration when performing in vitro assays to determine binding efficacy of targeted delivery systems, since performing these studies under flow resulted in a significant decrease of doxorubicin uptake when compared to studies in static conditions.

For this thesis, it is assumed that liposomes were internalized by cells through receptor-mediated endocytosis. To determine if doxorubicin uptake was specific to anti-PSMA ligand-receptor docking, cell lines were incubated with liposomes not targeting PSMA (either without a targeting ligand or labeled with an isotype control antibody). As shown in Table 1, the negative control studies using a static setup and flow setup, resulted in minimal uptake of doxorubicin when compared to the studies carried out with targeting liposomes. Therefore, the liposomal delivery system itself does not result in significant non-specific uptake by cells. This is key for

developing a delivery system that will not associate with cells unless they are specifically targeted, to minimize side effects and systemic toxicity.

## 2.8 LIMITATIONS OF STUDY

While this section attempts to observe how flow conditions will affect doxorubicin uptake by cells targeted via anti-PSMA liposomes, it is important to note that there are several limitations to this study. First of all the results showed better uptake by LNCaP and MatLu cells when compared to HUVEC, which would be the closest analogue to tumor-associated endothelial cells. HUVEC were induced to express PSMA by exposure to soluble factors present in tumor cell media, which is comparable to tumor vasculature development. However it was later demonstrated by the group, that there was a significant loss of PSMA expression in HUVEC as shown through immunohistochemistry studies before and after flow runs using conventional F12K media (not tumor-conditioned) (Figure 4-3). The studies presented in this section, were performed using the conventional media and resulted in low doxorubicin uptake by HUVEC, as these cells began to lose PSMA expression over the incubation time. It is expected that more favorable and realistic results would be obtained by replacing the media used in the flow runs with tumor-conditioned media.

# Chapter 3 EVALUATING GALA LIPOSOME FUSOGENICITY

## 3.1 RATIONALE

As previously discussed, a barrier to successful nanocarrier delivery is the tendency of the therapeutic agent to become entrapped within cellular compartments such as the endosome or within the nanocarrier itself. The delivery system presented in this thesis is designed to overcome the issue of nanocarrier entrapment by using a pH-responsive liposomal carrier, which will form membrane defects at acidic pH to allow the therapeutic to be released. The liposomes will also be functionalized with GALA fusogenic peptide, which will become activated at the acidic pH of the endosome to allow for fusion with the endosomal membrane and release of the therapeutic directly into the cytosol to bypass the issue of endosomal entrapment.

Although GALA has been previously conjugated on liposomes to obtain fusogenic delivery vesicles, there have been several issues with the system [38]. Primarily the fusogenicity has not been optimized to prevent activity at neutral pH, which would result in potential systemic issues from interactions with healthy cells. To address this, previous work has attached PEG on the surface of these vesicles to mask the GALA peptide during circulation and prevent unwanted fusion with healthy sites [38]. However this construct resulted in lowered fusogenic activity at acidic pH, which is a significant drawback as membrane fusion is necessary for the delivery system to function effectively. The liposomes discussed in this thesis, would overcome these issues by using a PEGylated pH-responsive membrane to obtain a carrier that would mask GALA during circulation to prevent fusion with healthy sites and expose GALA at acidic pH to enable fusogenic activity with the endosomal membrane. In addition by conjugating the anti-PSMA ligand on the surface of the liposome as discussed in Chapter 2, further selectivity can be achieved with the delivery system to minimize systemic toxicity issues.

## 3.2 OBJECTIVE

The aim of this study is to evaluate the fusogenicity of GALA-labeled vesicles by monitoring their ability to induce content leakage of endosomal analogue vesicles. This study is performed by systematically varying parameters on the GALA-labeled liposomal membrane to observe the effect on fusogenicity with the endosomal analogue vesicles.

## 3.3 HYPOTHESIS

The fusogenic peptide GALA can be conjugated on pH-responsive liposomes to obtain a pH-activated fusogenic response and the membrane parameters can be altered to tune fusogenicity of the GALA-labeled liposomes. In particular, GALA liposome-induced leakage from endosomal analogue vesicles will increase at acidic (pH≈5.0) incubation conditions compared to neutral pH.

## 3.4 MATERIALS AND METHODS

### 3.4.1 MATERIALS

The lipids L-α-phosphatidylcholine (Egg) (Egg-PC), 1,2-diheneicosanoyl-*sn*-glycero-3-phosphocholine (21PC), 1,2-distearoyl-sn-glycero-3-phosphate (monosodium salt) (DSPA), 1,2-dihexadecanoyl-sn-glycero-3-phosphate (sodium salt) (DPPA), 1,2-distearoyl-sn-glycero-3-phosphoethanolamine-N-[methoxy(polyethylene glycol)-2000] (ammonium salt) (DSPE-PEG), were purchased from Avanti Polar Lipids (Alabaster, AL) (all lipids at purity > 99%). Phosphate buffered saline (PBS), Sephadex G-50, Triton-X 100, ethylenediaminetetraacetic acid (EDTA), calcein (fluorexon, indicator grade) and cholesterol were obtained from Sigma-Aldrich (Atlanta, GA).

### 3.4.2 GALA PEPTIDE SYNTHESIS

GALA-lipid and free GALA peptide were obtained from Rutgers Chemical Biology Core Facility. Briefly, GALA peptide was synthesized on a Nautilus 2400 solid phase synthesizer (Argonaut Technologies, Redwood City, CA) and purified using a Prep LC 4000 Preparative Chromatography System (Waters Corporation, Milford, MA). The sample was then lyophilized on a Freezone 4.5 Plus Freeze Dry System (Labconco, Kansas City, MO).

For GALA-lipid, the free GALA was conjugated on 16:0 Succinyl PE (1,2-dipalmitoyl-*sn*-glycero-3-phosphoethanolamine-N-(succinyl) (sodium salt)) lipid before lyophilization. To incorporate the dried GALA-lipid in the liposome formulation, samples were first dissolved in 4:1 chloroform:methanol solution.

### 3.4.3 GALA LIPOSOME PREPARATION

The composition of GALA liposomes at a total of 10 µmoles lipid is shown in Table 2. As a negative control, liposomes were prepared of the same composition without GALA peptide. Lipids were dissolved in chloroform and mixed in a 25 ml round bottom flask. The chloroform was evaporated under vacuum for ten minutes at 55°C using a Buchi rotavapor R-200 (Buchi, Flawil, Switzerland) to obtain a lipid film. To ensure dryness, the film was then exposed to $N_2$ stream for 5 minutes. This film was then hydrated with 1 ml of 20 mM glycine (pH 9.0, 300 mOsm) and was annealed for 2 hours at 55°C in a water bath. The lipid suspension was then extruded 21 times through two stacked 200 nm polycarbonate membranes (Avestin Inc., Ottawa, Canada) in a water bath at 80°C. The lipid suspension was extruded again through 100 nm membranes. Vesicles were then passed through a 10 cm Sephadex G50 size exclusion chromatography (SEC) column and eluted with PBS (pH 7.4, 300 mOsm) to separate from the unentrapped glycine. The average size and zeta potential (ζ) of vesicle suspensions was

measured by dynamic light scattering using a Zetasizer Nano Z590 (Malvern Instruments, Worcester, UK).

**Table 2: COMPOSITION OF GALA-LABELED LIPOSOMES**

| Composition | Ratio | Lipids (10 µmole total) | PEG (mol %) | GALA (mol %) |
|---|---|---|---|---|
| A | 7:3 | egg-PC:cholesterol | 0 | 0.1 |
| B | 7:3 | DSPC:cholesterol | 0 | 0.1 |
| C | 8.57:0.95:0.48 | 21PC:DSPA:cholesterol | 0 | 0.1 |
| D | 8.57:0.95:0.48 | 21PC:DPPA:cholesterol | 0 | 0.1 |
| E | 8.57:0.95:0.48 | 21PC:DPPA:cholesterol | 1 | 0.1 |
| F | 8.57:0.95:0.48 | 21PC:DPPA:cholesterol | 1 | 0.3 |
| G | 8.57:0.95:0.48 | 21PC:DPPA:cholesterol | 3 | 0.3 |

### 3.4.4 ENDOSOMAL ANALOGUE VESICLE PREPARATION

For endosomal analogue vesicles, the composition chosen was 7:3 egg-PC:cholesterol. The vesicle preparation proceeded as above except the vesicles were hydrated in 75 mM calcein (pH 7.4, 300 mOsm). After annealing, the lipid suspension was then extruded 21 times through two stacked 100 nm polycarbonate membranes (Avestin Inc., Ottawa, Canada) at room temperature, 25 °C. Vesicles were then passed through a 10 cm Sephadex G50 SEC column and eluted with PBS (pH 7.4, 300 mOsm) to separate from the unentrapped calcein. The average size of vesicle suspensions was measured by dynamic light scattering using a Zetasizer Nano Z590 (Malvern Instruments, Worcester, UK).

### 3.4.5 CIRCULAR DICHROISM ANALYSIS

The circular dichroism (CD) spectra were collected on a J-710 Spectropolarimeter (Jasco Analytical Instruments, Easton, MD) in a sample chamber flushed with nitrogen at 23 °C. The θ values, expressed as degrees centimeter squared per decimole, were recorded. The value of the spectrum at 222 nm was analyzed to calculate % fractional alpha helicity [39].

Free GALA samples were prepared in 5 mM TES/100 mM KCL for CD analysis as previously described [40]. GALA was diluted into the buffer to obtain a 0.05 mg/ml solution and placed in capped quartz optical cells with 1 mm path length. GALA was scanned at various pH values ranging from 7.5 to 3.9, by addition of 0.2 M hydrochloric acid to the buffer solution. Studies were also performed in presence of lipid using the endosomal analogue vesicles described above, hydrated in PBS pH 7.4, for a final ratio of 50:1 lipid:peptide in the optical cell. The values of lipid only were subtracted to correct for the CD spectra of the lipid, these values were less than 5% of the intensity at 222 nm.

### 3.4.6 ENDOSOMAL ANALOGUE VESICLE LEAKAGE ANALYSIS

Endosomal analogue vesicles and GALA-labeled liposomes were incubated at a ratio of 2000:1 lipid:GALA at 25 °C in the dark. Samples at pH 7.4 were acidified by addition of hydrochloric acid drop-wise to obtain final pH values of 5.5, 5.0, and 4.5 (Figure 3-1). Negative control samples were also prepared by incubating endosomal analogue vesicles with liposomes of the same composition except not labeled with GALA.

Alliquots of each sample were pipetted into 2 mL of PBS (pH 7.4, 300 mOsm) in polystyrene cuvettes (1 mm path length) for a total of 0.30 µmole lipid. A Fluoromax-2 spectrofluorometer (Horiba Scientific, Edison, NJ) was used to measure calcein fluorescence ($\lambda_{excitation}$= 495 nm, $\lambda_{emission}$= 515 nm). These measurements were collected over 30 seconds, before ($I_b$) and after ($I_a$) addition of Triton-X 100 to determine the quenching efficiency ($Q_t = \frac{I_a}{I_b}$) at each time point ($t$). The % Quenching Efficiency ($\% \, QE$) was then calculated as follows:

$$\% \, QE = \frac{Q_t - Q_{min}}{Q_{max} - Q_{min}} \times 100$$

Where $Q_{max}$ is the maximum quenching efficiency of the pH 7.4 sample at the initial time point (t=0), and $Q_{min}$ is equal to unity. This methodology is accurate for calcein retention values above 13% of the initially encapsulated contents (75 mM) since relief of calcein self-quenching occurs essentially at concentrations below 10 mM [41] .

Finally the change in % Quenching Efficiency ($\Delta\%\ \mathrm{QE}$) is calculated as follows:

$$\Delta\%\ \mathrm{QE} = \frac{\%\ \mathrm{QE}_C - \%\ \mathrm{QE}_G}{\%\ \mathrm{QE}_G} \times 100$$

Where $\%\ \mathrm{QE}_C$ is the % Quenching Efficiency for the control sample with no GALA, and $\%\ \mathrm{QE}_G$ is the % Quenching Efficiency for the sample with GALA.

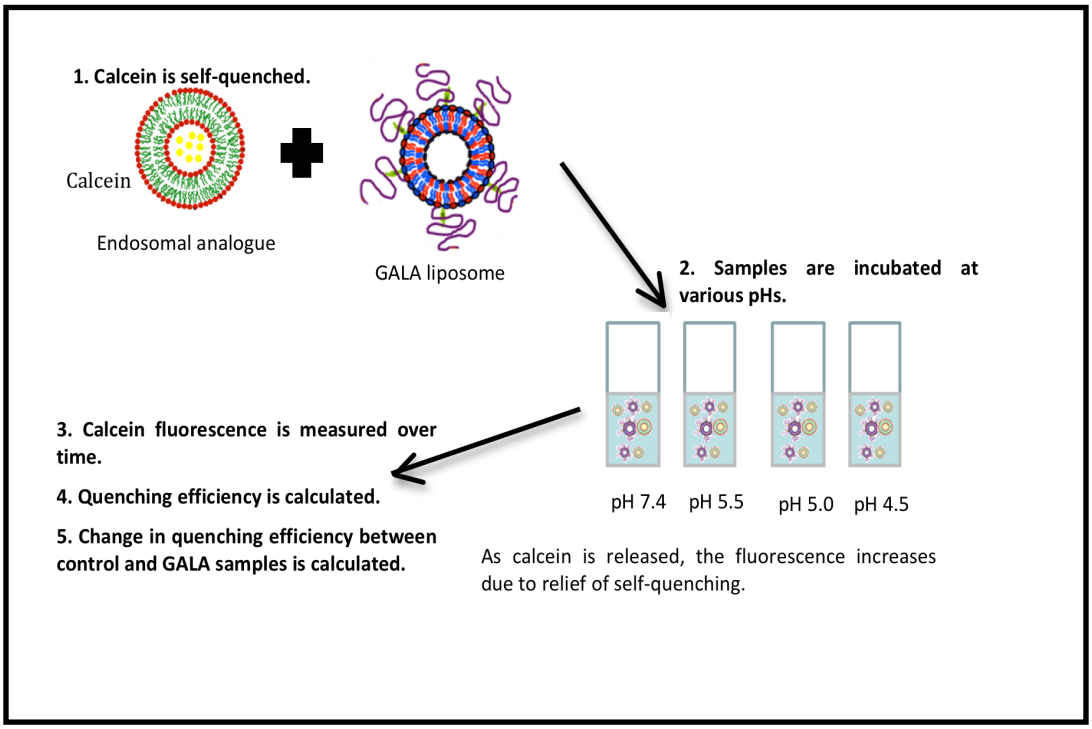


**Figure 3-1: ENDOSOMAL ANALOGUE LEAKAGE EXPERIMENTAL SETUP**

## 3.5 STATISTICAL ANALYSIS

Results are reported as the arithmetic mean of n independent measurements ± the standard deviation. ANOVA followed by Tukey's post-hoc test were used to calculate significant differences in the GALA-induced calcein leakage between different pH environments and compared to control setups. P-values less than 0.05 were considered to be significant.

## 3.6 RESULTS

### 3.6.1 FREE GALA PEPTIDE CHARACTERIZATION

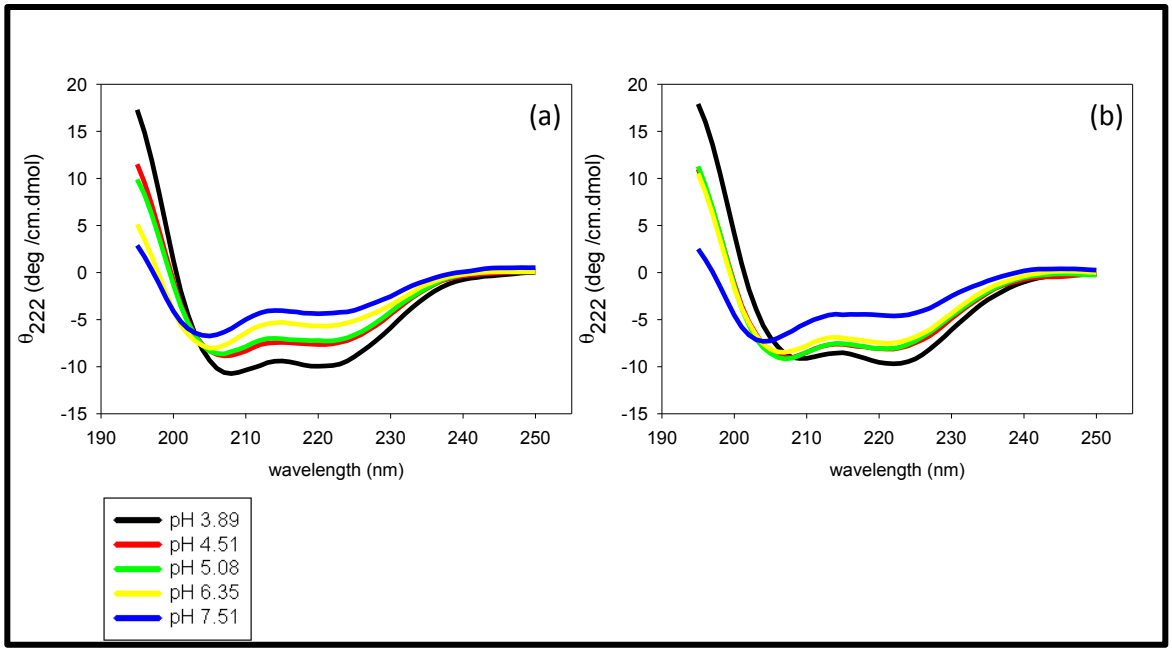


**Figure 3-2: REPRESENTATIVE CIRCULAR DICHROISM FOR FREE GALA PEPTIDE**
Free GALA peptide measured (a) in buffer and (b) in buffer containing 50:1 lipid:peptide.

Circular dichroism results were analyzed to determine alpha helicity of free GALA peptide at various pH values with and without presence of lipid. Since the band at 222 nm is related to the strong hydrogen-bonding environment of alpha helices the mean residue molar ellipticity at 222 nm was calculated using the following formula:

$$[\theta] = \frac{\theta \times 100 \times M}{C \times l \times n}$$

Where $\theta$ is the ellipticity in degrees, $l$ is the optical path in cm, $C$ is the concentration in mg/ml, $M$ is the molecular mass and $n$ is in the number of residues in the peptide. The mean residue molar ellipticity $[\theta]$ is given in deg.cm$^2$/dmol.

**Table 3: CIRCULAR DICHROISM MEASUREMENTS FOR FREE GALA AND FREE GALA INCUBATED WITH LIPID**

| pH | $[\theta]_{222}$ Liposome + Free GALA (deg.cm$^2$/dmol) | $[\theta]_{222}$ Free GALA (deg.cm$^2$/dmol) |
|---|---|---|
| 7.51 | -9328 ± 301 | -8705 ± 85 |
| 6.35 | -16428 ± 247 | -11420 ± 261 |
| 5.08 | -16291 ± 251 | -14672 ± 104 |
| 4.51 | -15148 ± 229 | -15305 ± 208 |
| 3.89 | -19595 ± 48 | -19964 ± 124 |

The % fractional helicity $(fH)$ was determined using the previously calculated mean residue molar ellipticity $[\theta]$ in the following formula [42]:

$$fH = \frac{[\theta]_{222} - 3000}{-36000 - 3000}$$

The circular dichroism results showed a 96.3% increase in alpha helicity from pH 7.51 to pH 3.89 for free GALA peptide in buffer, whereas there was an 83.3% increase when the peptide was in the presence of lipid. However, these values are not significantly different (p=0.108). At pH 5.08, a significant increase (p=0.00) in $[\theta]$ is observed when the GALA peptide is in the presence of egg-PC lipid vesicles compared to GALA peptide alone.

### 3.6.2 GALA LIPOSOME FUSOGENICITY

The GALA-liposome fusogenicity was monitored by systematically varying parameters on the targeting membrane, while monitoring the effect of these factors on endosomal analogue

leakage. The $\Delta\%\ QE$ was used to compare the extent of calcein leakage between the control and GALA samples.

#### 3.6.2.1 EFFECT OF MEMBRANE RIGIDITY

The effect of membrane rigidity was compared between compositions A and B (Table 2). Results at 60 minutes showed no significant difference in $\Delta\%\ QE$ between fluid membranes at room temperature (egg-PC:cholesterol) and gel membranes at room temperature (DSPC:cholesterol) at pH 4.5 or pH 7.4 (p= 0.958, 0.983).

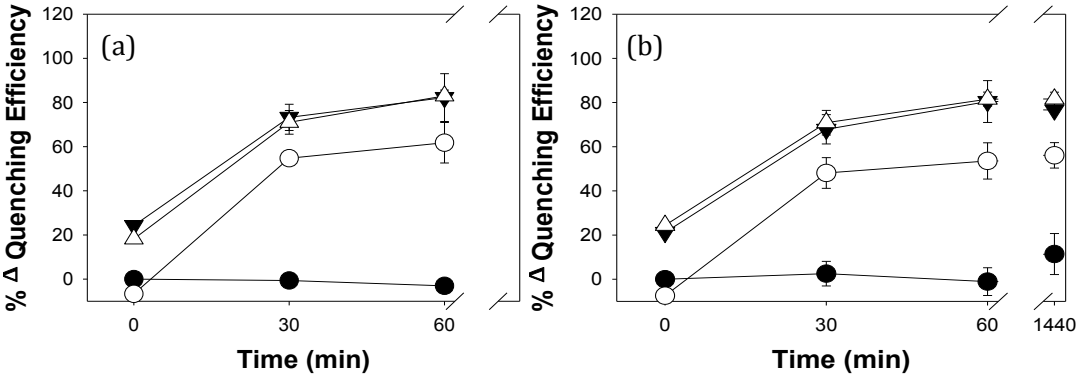


**Figure 3-3: EFFECT OF MEMBRANE RIGIDITY**
The $\Delta\%\ QE$ of (a) Composition A (egg-PC:cholesterol), fluid membrane and (b) Composition B (DSPC:cholesterol), rigid membrane. The GALA liposomes were incubated with endosomal analogue vesicles in PBS buffer at: (●) pH 7.4, (○) pH 5.5, (▼) pH 5.0, and (Δ) pH 4.5. The lines are guides to the eyes. Error bars represent standards deviations of repeated independent measurements (n = x).

#### 3.6.2.2 EFFECT OF HYDROCARBON CHAIN LENGTH OF TITRATABLE LIPID

The hydrocarbon chain length of the titratable lipid (PA) was varied between compositions C (containing DSPA: 18 carbon chain length) and D (containing DPPA: 16 carbon chain length) (Table 2). Results showed a significant difference in %Δ QE induced by GALA liposomes composed of DSPA compared to DPPA (p=0.01, at time 60 min for pH 4.5), where % Δ QE = 75.22% for composition C and % Δ QE = 22.52% for composition D.

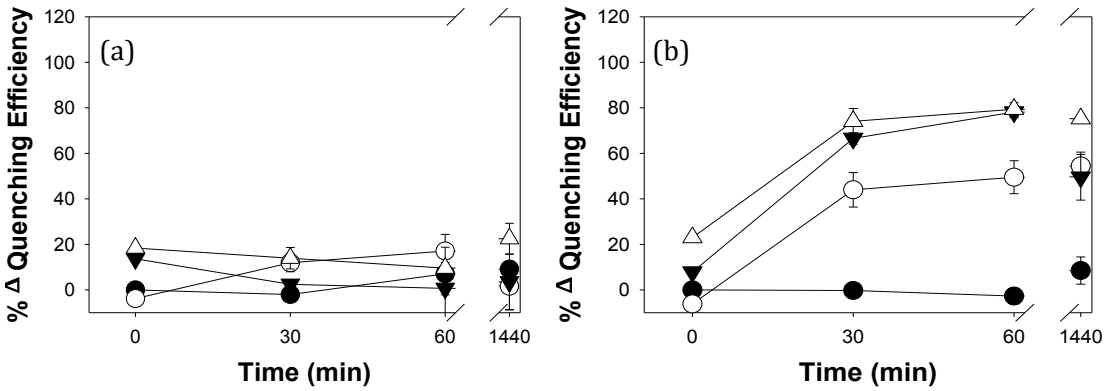


**Figure 3-4: EFFECT OF HYDROCARBON CHAIN LENGTH OF TITRATABLE LIPID**
The $\Delta\% \, QE$ of (a) Composition C (21PC:DSPA) and (b) Composition D (21PC:DPPA). The GALA liposomes were incubated with endosomal analogue vesicles in PBS buffer at: (●) pH 7.4, (○) pH 5.5, (▼) pH 5.0, and (Δ) pH 4.5. The lines are guides to the eyes. Error bars represent standards deviations of repeated independent measurements (n = x).

### 3.6.2.3 EFFECT OF GALA GRAFTING DENSITY

The effect of GALA grafting density was observed by comparing 0.1 mol% GALA on pH-responsive liposome composition E (21PC:DPPA:cholesterol, 1 mol% PEG) with 0.3 mol% GALA on liposome composition F (Table 2). The increase in GALA concentration resulted in increased % Δ QE at all pH values. Comparing composition E with composition F, the % Δ QE increased by 81.3% at pH 7.4 and by 72.7% at pH 4.5 after a 24-hour incubation.

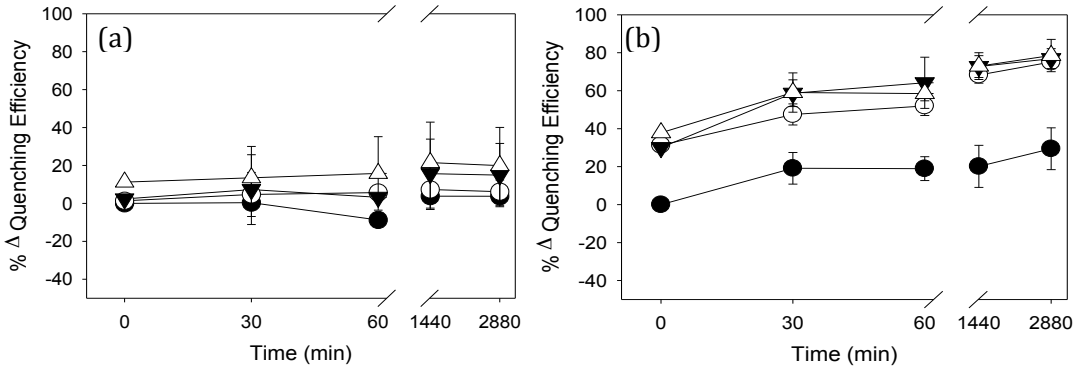


**Figure 3-5: EFFECT OF GALA GRAFTING DENSITY**
The $\Delta\%\ QE$ of (a) Composition E (0.1 mol% GALA) and (b) Composition F (0.3 mol% GALA). The GALA liposomes were incubated with endosomal analogue vesicles in PBS buffer at: (●) pH 7.4, (○) pH 5.5, (▼) pH 5.0, and (Δ) pH 4.5. The lines are guides to the eyes. Error bars represent standards deviations of repeated independent measurements (n = x).

### 3.6.2.4 EFFECT OF PEG GRAFTING DENSITY

The PEG grafting density was increased from composition F (1 mol% PEG) to composition G (3 mol% PEG) to attempt to minimize fusogenic activity at neutral pH. The results after a 48 hour incubation showed no change in % Δ QE for both compositions at acidic pH of 4.5 (p=1.0) while achieving a decrease in % Δ QE at the neutral pH of 7.4 (p=0.239)

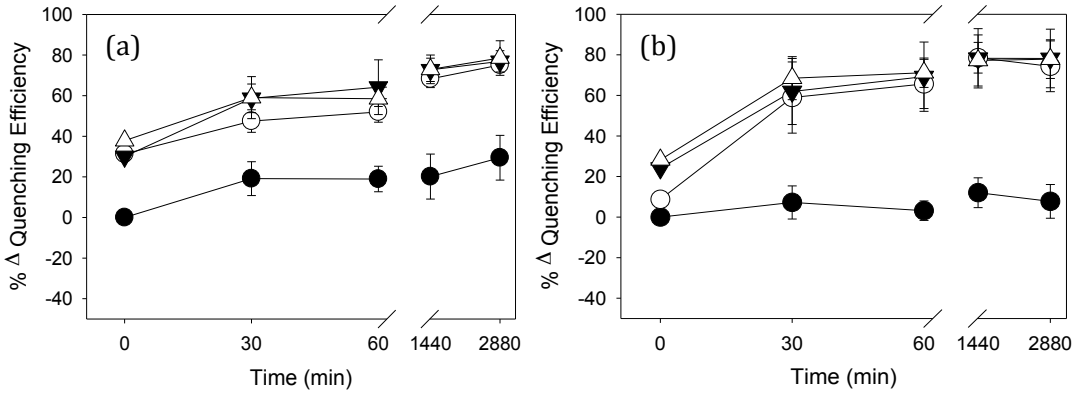


**Figure 3-6: EFFECT OF PEG GRAFTING DENSITY**
The $\Delta\%\ QE$ of (a) Composition F (1 mol% PEG) and (b) Composition G (3 mol% PEG). The GALA liposomes were incubated with endosomal analogue vesicles in PBS buffer at: (●) pH 7.4, (○) pH 5.5, (▼) pH 5.0, and (Δ) pH 4.5. The lines are guides to the eyes. Error bars represent standards deviations of repeated independent measurements (n = x).

## 3.7 DISCUSSION

### 3.7.1 ALPHA HELICAL CONTENT OF FREE GALA PEPTIDE INCREASED BY ACIDIC PH

First, free GALA was characterized to observe if the peptide in free form behaved as expected. From the circular dichroism results (Figure 3-2), it is clear that free GALA does exhibit pH-dependent activation by showing increasing alpha-helicity with buffer acidification. When these results are compared to free GALA peptide that was incubated with lipid vesicles, the same trend was observed. At pH 5.08 the significant decrease in $[\theta]_{222}$, which corresponds to increased alpha helicity, observed when the GALA peptide is in the presence of egg-PC lipid vesicles compared to GALA peptide alone suggests that GALA is interacting with the lipid bilayer [40]. However, at more acidic pH values the alpha helical fraction is not significantly affected by the presence of lipid vesicles. These findings suggest that when GALA is incubated with lipid vesicles the alpha-helical conformation extent as a function of pH is enhanced, with differences observable at pH 5.0 where the peptide first becomes activated. However upon further acidification, the differences become negligible.

### 3.7.2 GALA LIPOSOME FUSOGENICITY INDEPENDENT OF MEMBRANE RIGIDITY

Comparing Composition A (eggPC:cholesterol, fluid membrane) with Composition B (DSPC:cholesterol, rigid membrane), there was no observable difference between %ΔQE of the samples at all pH values and time points. Therefore the membrane rigidity of the GALA liposome does not significantly affect induced endosomal analogue content leakage. This is an important finding since rigid membranes are more stable during circulation in-vivo.

### 3.7.3 MEMBRANE DEFECTS ON GALA LIPOSOME AFFECT FUSOGENIC ABILITY

The rigidity of Composition C (21PC:DSPA) membranes compared to Composition D (21PC:DPPA) membranes does not differ greatly and furthermore results showed no difference in

fusogenicity for membrane compositions of varying rigidity (Composition A vs. B). Therefore the stark difference in fusogenicity when DPPA was substituted for DSPA may be due to another factor in the liposomal design. One possible mechanism is depicted in Figure 3-7, where the difference in hydrocarbon chain length of the negatively charged lipid determines the extent of membrane heterogeneity. Due to increased van der Waals bonding strength upon acidification between domains composed of 18-carbon chain length lipid (DSPA) when compared to 16-carbon chain length (DPPA) domains, the more compacted DSPA domains could result in more pronounced membrane defect at the interface between the DSPA and 21-PC domains. It is possible that when GALA peptide is activated and converts to an alpha-helix conformation, it preferentially imbeds within the defects on its own membrane or defects on neighboring targeting vesicles, and is therefore not available to bind to the endosomal analogue vesicles and induce content leakage. This preferential binding affinity of activated GALA to the pronounced membrane defects could be due to a lower conformational energy required for GALA to bind to these membrane defects as opposed to endosomal analogue membranes, or due to exposure of hydrophobic lipid areas at the interfacial membrane defects to the water environment which are screened by the peptide-membrane association.

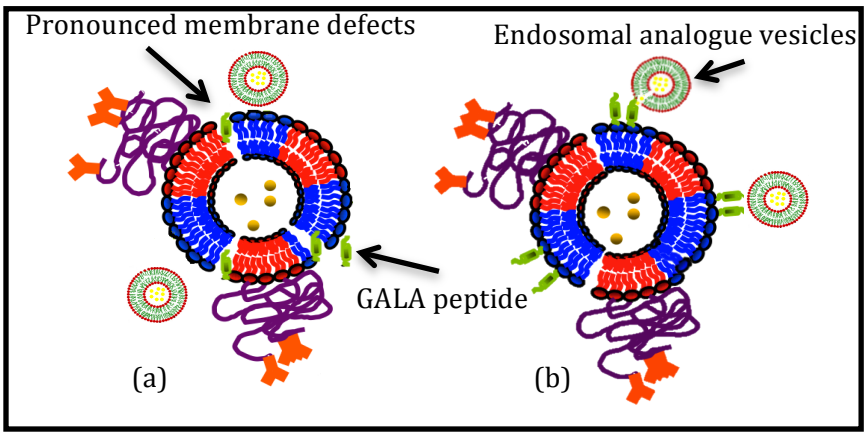


**Figure 3-7: PROPOSED MECHANISM OF GALA LIPOSOME FUSOGENICITY**
Proposed mechanism of GALA liposome fusogenicity for (a) Composition C, 21PC:DSPA, and (b) Composition D, 21PC:DPPA. GALA peptide in composition D is available to bind to the endosomal analogue vesicles since the membrane defects are not as pronounced as those in composition C. *Schematic is not drawn to scale.

### 3.7.4 GALA LIPOSOME FUSOGENICITY DEPENDENT ON GALA AND PEG GRAFTING DENSITY

As expected, GALA liposome fusogenicity was dependent on many parameters of the liposomal membrane. Results showed that increasing GALA grafting density from 0.1 mol% to 0.3 mol% (Compositions E and F) resulted in a significant increase in GALA-induced endosomal analogue leakage. Although an increase in fusogenic behavior at acidic pH is required to effectively allow endosomal escape, it is also necessary to maintain low activity at neutral pH to ensure minor interaction of the delivery system with healthy tissues during circulation in-vivo. Therefore, the PEG grafting density was increased from 1 mol% to 3 mol% (Compositions F and G) to mask the peptide more effectively during circulation at neutral pH. The results obtained showed a significant decrease in activity at pH 7.4 while maintaining fusogenic activity at pH 4.5, therefore the fusogenicity can be controlled during neutral pH and activated only by acidic pH environments.

## 3.8 LIMITATIONS OF STUDY

Preliminary work observing the effect of GALA activation by pH acidification to induce leakage of endosomal analogue vesicles showed promising results; however there are certain limitations with the studies performed. One limitation with this study stems from the difference in diameter between the endosomal analogue vesicles chosen for the study (~100 nm) and endosomes in-vivo (~500 nm) [43]. This is important as fusogenicity of membranes is dependent on vesicle size [44], however for this work the preliminary results obtained were sufficient to observe the behavior of GALA liposome activity. In the future, studies in-vitro can be performed to observe the fusogenic activity of GALA liposomes on endothelial cell endosomes.

An additional limitation in this study is due to the pH dependence of calcein fluorescence [45]. The change in fluorescence with pH was addressed by ensuring that all fluorescence

measurements were taken at neutral pH since it was shown that calcein fluorescence change was reversible. A more controlled study could be performed by encapsulating a fluorescent molecule that is not affected by the pH range of interest. One such option is ANTS/DPX, however attempts to encapsulate either probe in the pH-responsive GALA liposomes resulted in minimal encapsulation efficiency, which could be due to incompatibilities between the negatively charged liposomes and the fluorescent molecules.

# Chapter 4 SUMMARY AND FUTURE WORK

## 4.1 SUMMARY

Using pH-responsive liposomes, the work presented in this thesis is divided into two sections: (1) PSMA-targeting under static and flow conditions and (2) GALA liposome fusogenicity. Results showed that it was possible to maintain PSMA-targeting in-vitro under static and flow conditions and that liposomes labeled with GALA displayed pH-responsive fusogenic behavior. However, the ultimate goal of this research is to develop a drug delivery system for antivascular therapy that encompasses both components of this thesis.

### 4.1.1 PROPOSED MECHANISM OF DRUG DELIVERY

The system that is envisioned (Figure 4-1) will be constructed of liposomes that are functionalized with targeting ligands to provide specificity to tumor-associated endothelial cells. The therapeutic is encapsulated during circulation in the neutral pH of the blood to spare healthy sites, and the release is pH-triggered after uptake into the acidic environment of the targeted endosome. The delivery mechanism is initiated when the targeting ligand docks at the receptor site resulting in receptor-mediated endocytosis of the liposomes. Upon uptake, the liposomes become activated to fuse with the endosomal membrane and prevent endosomal entrapment. Since the liposomal membrane is also pH-triggered, this should result in a burst release of the encapsulated therapeutics directly into the cytosol of the cell. Cytosolic release of the cargo increases the bioavailability of the therapeutic, resulting in improved therapeutic efficacy. Therefore this system has the potential to decrease the required administered dose, while still obtaining the desired antivascular therapeutic effect.

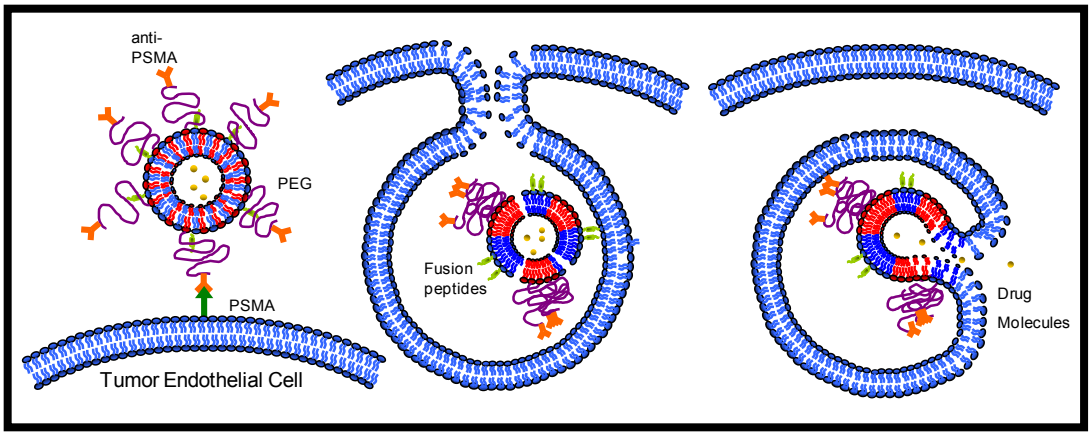


**Figure 4-1: PROPOSED MECHANISM OF DRUG DELIVERY**

## 4.2 FUTURE WORK

Although preliminary studies have been performed to understand how membrane properties affect the fusogenicity of GALA conjugated on the liposomal surface, future work is necessary to optimize the system and to further characterize the fusogenic mechanism. For example, membrane properties need to be optimized to minimize activity at neutral pH while maintaining activity at acidic pH. This could be attained by tuning membrane properties such as: PEG grafting density, GALA grafting density, and lipid composition. The goal is to obtain a system that is only fusogenically-active when necessary, resulting in endosomal escape of therapeutics and minimal systemic toxicity by preserving healthy sites.

Future studies to observe endosomal fusion in vitro can be performed by incubating fluorescently tagged anti-PSMA GALA liposomes with cells expressing PSMA. Imaging can be utilized to determine the extent of GALA-induced endosomal membrane fusion. Further studies can be performed with doxorubicin-loaded vesicles, where the fluorescence of doxorubicin can be imaged to observe the location of the delivery within the cell. For example, it would be

possible to determine if the GALA liposomes are releasing the therapeutic within the cytosol of the cell or if the therapeutic remains entrapped within the endosomal compartment.

In addition, the therapeutic efficacy of GALA liposomes needs to be compared to conventional liposomes. Cell viability assays measured by live/dead staining can be performed in vitro to determine cytotoxicity of pH-responsive GALA liposomes compared to pH-responsive liposomes not containing GALA, as well as liposomes without GALA and without pH-responsive membranes.

Finally, future studies need to be performed to optimize the kinetics of the system. For the delivery mechanism to be effective, the fusogenicity of GALA with the endosomal membrane needs to be tuned with the release time of the therapeutic. GALA should fuse with the endosomal membrane before the majority of the therapeutic contents are released to ensure that the therapeutic is released into the cytosol of the cell and not degraded by the acidic pH environment. The kinetics can be altered to achieve such a release by tuning membrane properties such as the ratio of negatively charged lipid to zwitterionic lipid to vary the size of domains, or the carbon tail mismatch to vary the severity of the membrane defects. Optimizing the membrane properties would effectively control the release of the therapeutic from the liposome, and allow it to be properly timed with the fusogenicity of GALA with the endosomal membrane to obtain therapeutic delivery to the cytosol for increased bioavailability and cytotoxicity.

# APPENDIX

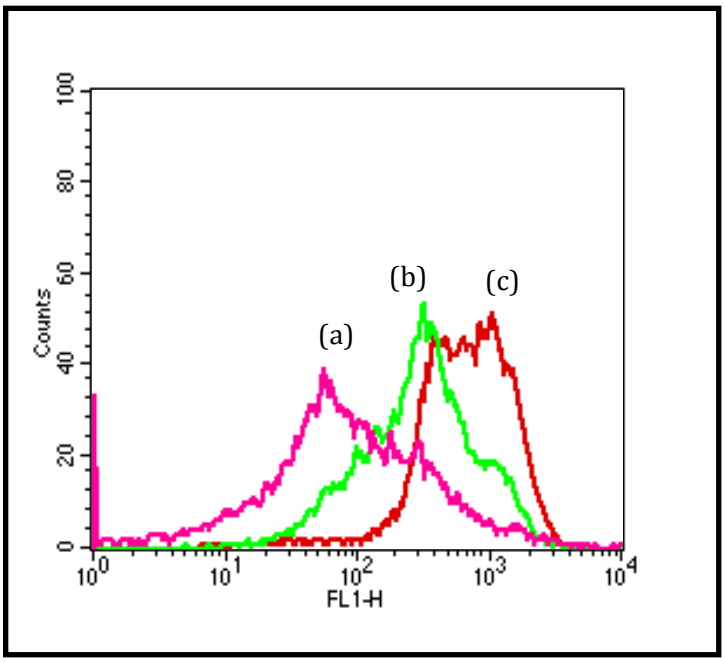


**Figure 4-2: RELATIVE EXPRESSION OF PSMA ACROSS CELL LINES**
Immunohistochemistry analysis of PSMA-expressing cell lines, depicting relative expression of PSMA. *Collected by Dr. Amey Bandekar, Rutgers University.

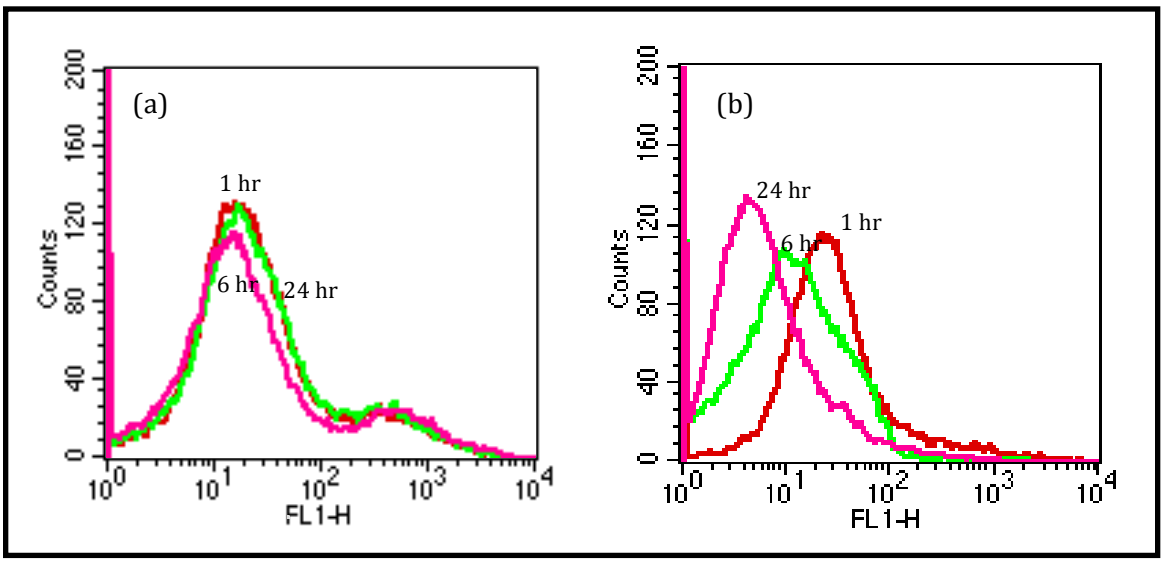


**Figure 4-3: PSMA EXPRESSION OF PSMA-INDUCED HUVEC UNDER FLOW**
Immunohistochemistry analysis of PSMA-expressing HUVEC under flow after 1 hr, 6 hr, and 24 hr incubation using (a) tumor-conditioned media and (b) conventional RPMI media. *Collected by Dr. Amey Bandekar, Rutgers University.

# REFERENCES


1. Howlader, N., et al., *SEER Cancer Statistics Review, 1975-2008*, 2011, National Cancer Institute, Bethesda, MD.
2. Folkman, J., *Angiogenesis in cancer, vascular, rheumatoid, and other disease.* Nat Med, 1995(1): p. 27-31.
3. SIemann, D., *The Unique Characteristics of Tumor Vasculature and Preclinical Evidence for its Selective Disruption by Tumor-Vascular Disrupting Agents.* Cancer Treat Rev., 2011. **37**(1): p. 63-74.
4. Vaklavas, C., Lenihan, D., Tsimbueridou, A., *Anti-Vascular Endothelial Growth Factor Therapies and Cardiovascular Toxicity: What Are the Important Clinical Markers to Target?* The Oncologist Cancer Biology, 2010(15): p. 130-141.
5. Jain, R., Duda, D., Clark, J., Loeffler, J., *Lessons from phase III clinical trials on anti-VEGF therapy for cancer.* Nature Clinical Practice Oncology, 2006. **3**(1): p. 24-40.
6. Noguchi, Y., et al., *Early phase tumor accumulation of macromolecules: A great difference between the tumor vs.normal tissue in their clearance rate.* Jpn. J. Cancer Res., 1998. **89**: p. 307-314.
7. O'Brien, M., Wigler, N., Tendler, C., *Reduced cardiotoxicity and comparable efficacy in a phase III trial of pegylated liposomal doxorubicin HCl (CAELYX™/Doxil®) versus conventional doxorubicin for first-line treatment of metastatic breast cancer.* Annals of Oncology, 2004. **15**(3): p. 440-449.
8. Apostolidou, E., Cores, J., Tsimberidou, A., Giles, Francis., *Pilot study of gemtuzumab ozogamicin, liposomal daunorubicin, cytarabine and cyclosporine regimen in patients with refractory acute myelogenous leukemia.* Leukemia Research, 2003. **27**(10): p. 887-891.
9. Stathopoulos, G., Boulikas, T., Vougiouka, M., Stathopulous, J., *Pharmacokinetics and adverse reactions of a new liposomal cisplatin (Lipoplatin): Phase I study.* Oncology Reports, 2005. **13**: p. 589-595.
10. Torchilin, V., *Recent advances with liposomes as pharmaceutical carriers.* Nature Reviews Drug Discovery, 2005. **4**: p. 145-160.
11. Karve, S., et al., *The use of pH-triggered leaky heterogeneities on rigid lipid bilayers to improve intracellular trafficking and therapeutic potential of targeted liposomal immunochemotherapy.* Biomaterials, 2009. **30**: p. 6055-6064.
12. Bandekar, A., et al., *Antitumor efficacy following the intracellular and interstitial release of liposomal doxorubicin.* Biomaterials, 2012. **33**: p. 4345-4352.
13. Karve, S., Kempegowda, G., Sofou, S., *Heterogeneous domains and membrane permeability in phosphatidylcholine- phosphatidic acid rigid vesicles as a function of pH and lipid chain mismatch.* Langmuir, 2008. **24**: p. 5679-88.
14. Bhagat, M., Sofou, S., *Heterogeneous domains and membrane fusogenicity in phosphatidylcholine- phosphatidic acid rigid vesicles as a function of pH and lipid chain mismatch.* Langmuir, 2010. **26**: p. 1666-1673.
15. Mozafari, M., *Bioactive Entrapment and Targeting Using Nanocarrier Technologies: An Introduction*. Nanocarrier Technologies: Frontiers of Nanotherapy. 2006, Netherlands: Springer.
16. Li, W., Nicol, F., Szoka, F., *GALA: a designed synthetic pH-responsive amphipathic peptide with applications in drug and gene delivery.* Advanced Drug Delivery Reviews, 2004. **56**: p. 967-985.

17. Taraboletti, G., Margosio, B., *Antiangiogenic and antivascular therapy for cancer.* Curr Opin Pharmacol, 2001. **1**(4): p. 378-384.
18. Liu, H., et al., *Constitutive and antibody-induced internalization of prostate-specific membrane antigen.* Cancer Res, 1988. **58**: p. 4055-60.
19. Hayes, A., Li, L., Lippman, M., *Anti-vascular therapy: a new approach to cancer treatment.* Best Practice, 2000. **172**: p. 39-42.
20. Chang, S., O'Keefe, S., Bacich, D., et al., *Prostate-specific Membrane Antigen Is Produced in Tumor-associated Neovasculature.* Clinical Cancer Research, 1999. **5**: p. 2674-2681.
21. Silver, D., Pellicer, I., Cordon-Cardo, C., *Prostate-specific membrane antigen expression in normal and malignant human tissues.* Clinical Cancer Research, 1997. **3**(1): p. 81-85.
22. Israeli, R.S., Powell, C. T., Corr, J. G., Fair, W. R., and Heston, W. D. , *Expression of the prostate-specific membrane antigen.* Cancer Research, 1994. **54**: p. 1807-1811.
23. Olson, W., Heston, W., Rajasekaran, A., *Clinical Trials of Cancer Therapies Targeting Prostate-Specific Membrane Antigen.* Reviews on Recent Clinical Trials, 2007. **2**: p. 182-190.
24. Lupold, S., Hicke, B., Lin, Y., Coffey, D. , *Identification and characterization of nuclease-stabilized RNA molecules that bind human prostate cancer cells via the PSMA.* Cancer Research, 2002. **62**: p. 4029-4033.
25. Primeau, A.J., Rendon, A., Hedley, D., Tannock, I., *The distribution of the anticancer drug doxorubicin in relation to blood vessels in solid tumors.* Clinical Cancer Research, 2005. **11**: p. 8782-8788.
26. Gabizon, A., Martin, F., *Polyethylene glycol-coated (pegylated) liposomal doxorubicin. .* Drugs, 1997. **54**(4): p. 15-21.
27. Kilickap, S., Akgul, E., Aksoy, S., Barista, I., *Doxorubicin-induced second degree and complete atrioventricular block.* Europace, 2005. **7**: p. 227-230.
28. Straubinger, R., Arnold, R., Zhou, R., Mazurchuk, R., Slack, J., *Antivascular and Antitumor Activities of Liposome-associated Drugs.* Anticancer Research, 2004. **24**: p. 397-404.
29. Horoszewicz JS, L.S., Kawinski E, Karr JP, Rosenthal H, Chu TM, Mirand EA, Murphy GP., *LNCaP model of human prostatic carcinoma.* Cancer Research, 1983. **43**(4): p. 1809-1818.
30. Kouvroukoglou S, L.C., Wallace JD, Zygourakis K, Epner DE., *Bioenergetics of rat prostate cancer cell migration.* Prostate, 1998. **34**(2): p. 137-144.
31. Liu, T., et al., *Detection of prostate-specific membrane antigen on HUVECs in response to breast tumor-conditioned medium.* Int J Oncol, 2011. **38**(5).
32. Kolhar, P., Anselmo, A,. Gupta, V., et al., *Using shape effects to target antibody-coated nanoparticles to lung and brain endothelium.* PNAS, 2013. **110**(26): p. 10753-10758.
33. Gabizon, A. and D. Papahadjopoulos, *Liposome formulations with prolonged circulation time in blood and enhanced uptake by tumors.* PNAS, 1988. **85**: p. 6949-6953.
34. Sofou, S., et al., *Engineered liposomes for potential a-particle therapy of metastatic cancer.* J Nucl Med, 2004. **45**.
35. Smith-Jones, P.e.a., *In Vitro Characterization of Radiolabeled Monoclonal Antibodies Specific for the Extracellular Domain of Prostate-specific Membrane Antigen.* Cancer Res, 2000. **60**: p. 5237-5243.
36. Bagalkot, V., Farokhzad, O.C., Langer, R., Jon, S., *An Aptamer–Doxorubicin Physical Conjugate as a Novel Targeted Drug-Delivery Platform.* Angew Chem Int Ed Engl, 2006. **45**(48): p. 8149-8152.

37. Wu, X., Ding, B., Gao, J., Gao, S., *Second-generation aptamer-conjugated PSMA-targeted delivery system for prostate cancer therapy.* International Journal Nanomedicine, 2011. **6**: p. 1747-1756.
38. Etzerodt, T., Trier, S., Henriksen, J., Andresen, T., *A GALA lipopeptide mediates pH- and membrane charge dependent fusion with stable giant unilamellar vesicles.* Soft Matter, 2012. **8**(21): p. 5933-5939.
39. Correa, D., Ramos, C., *The use of circular dichroism spectroscopy to study protein folding, form and function.* African Journal of Biochemistry Research, 2008. **3**(5): p. 164-173.
40. Subbarao, N., Parente, RA., Szoka, FC., Nadasdi, L., Pongracz, K., *pH-dependent bilayer destabilization by an amphipathic peptide.* Biochemistry, 1987(26): p. 11.
41. Karve S., A.A., Zhou Y., Rotolo J., Sofou S. , *The use of pH-triggered leaky heterogeneities on rigid lipid bilayers to improve intracellular trafficking and therapeutic potential targeted liposomal immunochemotherapy.* Biomaterials, 2009. **30**: p. 6055-6064.
42. Morriset, J., David, JS., Pownall, HJ., Gotto, AM., *Interaction of an apolipoprotein (apoLP-alanine) with phosphatidylcholine.* Biochemistry, 1973. **12**: p. 1290-1299.
43. al., G.e., *Rab9 GTPase Regulates Late Endosome Size and Requires Effector Interaction for its Stability.* Molecular Biology of the Cell, 2004. **15**(12): p. 5420-5430.
44. Parente, R., Nir, S., Szoka, F., *pH-dependent Fusion of Phosphatidylcholine Small Vesicles.* The Journal of Biological Chemistry, 1988. **263**(10): p. 4724-4730.
45. FluoroProbes. *Calceins*. 2008; Available from: http://www.interchim.fr/ft/4/466251.pdf.